UKAEA-CCFE-CP(25)12

M Maslov, D Kos, Z Ghani, A Milocco, Z Huang, B Gray, JET contributors

Radiation effect in optical fibres measured in fusion environment

Radiation effect in optical fibres measured in fusion environment

M Maslov, D Kos, Z Ghani, A Milocco, Z Huang, B Gray, JET contributors

This paper has been submitted to
33rd Symposium on Fusion Technology (SOFT), Dublin, Ireland, 22 - 27 September 2024

Radiation effects in optical fibres measured during JET DT plasma experiments

M Maslov[1], D Kos[1], Z Ghani[1], A Milocco[2], Z Huang[1], B Gray[1], I. Ipatova[1], the JET contributors and the EUROfusion Tokamak Exploitation Team***

[1]UKAEA, Culham Campus, OX143DB, United Kingdom
[2]ISIN, Via Capitan Bavastro, 116 – 00154 Roma, Italy
** see the author list of C.F. Maggi et al 2024 Nucl. Fusion 64 112012 doi 10.1088/1741-4326/ad3e16*
*** see the author list of E. Joffrin et al 2024 Nucl. Fusion 64 112019 doi 10.1088/1741-4326/ad2be4*

Abstract: In 2021 and 2023 JET has completed experiments with D/T plasma mixtures where a significant amount of 14 MeV neutrons were released. To collect experimental data on the effect of fusion relevant radiation environment on optical fibres, a 60 metres long pure fused silica fibre has been coiled and placed in the vicinity of the JET machine to accumulate neutron and gamma dose during these experiments. Existing high-OH content radiation resistant fibres were used to connect the sample fibre with the lab space outside the neutron shield, so that the change in optical properties could be measured remotely in real time during and between JET plasma pulses. Significant amount of data was collected over that period. Radiation-induced emission (RIE) was observed over the whole measured spectrum but was dominant in the blue range. Prompt radiation-induced attenuation (RIA) is also dominant the blue range of spectrum and very weak in the near-infrared. The majority of the short-term radiation-induced damage recovers within 1 hour after the irradiation, but a fraction of the transmission loss remained permanent.

Introduction: As fusion devices transition from smaller research facilities to larger nuclear capable machines, plasma diagnostics and control instruments must evolve to cope with the new constraint – radiation environment. Neutron and gamma radiation is known to have deleterious effects on the properties of optical components, and the optical fibres are especially vulnerable.

Heating of the fibres to 250-400°C is known to reduce the radiation induced absorption by thermal annealing. This method was validated during DT experiments in TFTR [1] and then implemented in several diagnostics on JET [2]. Tolerance to radiation can be further improved through the manufacturing techniques, such as doping of fibres and/or cladding with various impurities. High-OH content fibres are well known to be more resistant to radiation induced absorption than pure SiO_2 fibres, but other types of doping are also being studied [3-5].

Introduction of impurities into fibres can affect their optical transmission and may not be suitable for some diagnostic applications. In particular, Thomson Scattering diagnostic such as the one developed for ITER relies on efficient transmission of low-level light signal over the broad range of visible and near-infrared spectrum, and no optimal solution for the fibres has been found [6]. Provisionally, it is planned to use moderate level of OH-doping in the fibres exposed to radiation to find a compromise between the intrinsic transmission loss caused by the doping and the radiation-induced absorption.

At JET, the High Resolution Thomson Scattering (HRTS) diagnostic implements optical fibres, and approximately 10 metres of length for each spatial point is located inside the biological shield and subject to neutron irradiation [7]. These fibres remain at ambient temperature ~20°C as no in-situ heating could be implemented.

The purpose of the work reported here is two-fold: 1) collect experimental data on the effect of fusion neutrons/gammas on the fibres which are used for the HRTS in a controlled manner to be able to correct the diagnostic data if required, and 2) document the effects for the benefit of diagnostics on other fusion machines.

A 60 metres long fused silica fibre has been coiled and placed near one of the main horizontal ports at JET where the relative ease of access was available together with high neutron fluxes. To measure the optical properties of the fibre during and after the irradiation, it was connected to the already available OH-doped fibres [8] which provided the transfer of light signal from the vicinity of JET to the lab space outside of the biological shield. Four OH-doped fibres were used: two provided the light transfer to and from the fused silica fibre at JET, and the other pair was connected on the JET side to provide reference measurement. Each OH-doped fibre had about 35 metres long end within the JET biological shield (70 metres for two connected fibres), thus the total length was comparable to the sample fibre but with somewhat lower neutron fluence due to their location. All the measurements were done at the ambient temperature ~20°C, i.e. no heating of the fibres was implemented.

Optical transmission in this setup was measured with a broadband light source connected to the input fibre and a compact spectrometer at the output. The light source was on continuously during the measurements except in a few plasma pulses where it was deliberately powered off to only measure the radiation induced emission. The compact spectrometer was controlled by a PC and produced one spectrum every second for 10 minutes during and after JET plasma pulses. Typical JET pulse lasts 60-80 seconds, with the actual plasma starting from the 40s timer. In this work, the time base has not been adjusted to show plasma initiation at 0s, as is usually done for publication of JET data, since the measurements with respect to the absolute time shown by the Central Timing System are important for discussion of results later in this paper. Duration of the plasma varied between 20 and 40 seconds, and the high neutron irradiation phase would typically last between 1 and 6 seconds. Therefore, each fibre measurement (600 spectra in 10 minutes) contained sufficient data pre-irradiation as reference, several frames during irradiation, and then around 9 minutes post-irradiation evolution. The data for each frame came out as intensity versus wavelength, in the range of λ=450-1100nm. Figure 1 shows example of the measured spectrum at the beginning and at the end of the DT campaigns. OH-doping in the transmission fibres causes characteristic transmission losses at certain wavelengths, thus there are dips near λ=723nm, λ=877nm and especially at λ=930-970nm where the transmitted signal was reduced to zero.

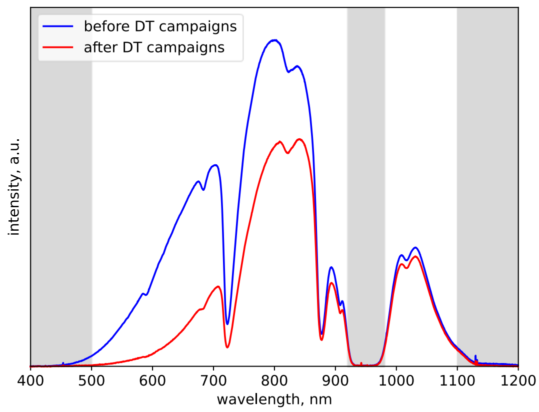

Figure 1: Measurement of the probing light spectrum through the experimental setup, taken at the beginning of DTE2 (blue) and at the end of DTE3 (red). Greyed out spectral intervals are not considered for the analysis.

The timeline of the measurements is outlined in table 1. The DTE2 campaign lasted approximately 5 months between Aug.2021 and Dec.2021, with ~700 pulses and **8.48*10^{20}** 14MeV neutrons released. Between Jan.2022 and Sep.2023 only experiments with pure deuterium were performed.

DTE3 campaign took place between Sept-Oct 2023 (~1.5 months), with ~570 pulses and **7.3*10^{20}** 14MeV neutrons released. Further pure deuterium plasmas were produced between Oct-Dec 2023 and then JET operations finished. The irradiated fibre has been recovered from JET in June 2024 for ex-situ measurements, ~8 months after the end of DTE3.

Period	Pulse range	Duration	14MeV neutrons	2.45MeV neutrons
DTE2 campaign	99294-99982	5 months	8.48*10^{20}	-
Isotope cleanup and D-D experiments	99983-104126	20 months	-	4.9*10^{19}
DTE3 campaign	104127-104697	1.5 months	7.31*10^{20}	-
Isotope cleanup and last D-D experiments	104698-105929	2.5 months	-	2.0*10^{19}
Rest time until fibre removal	-	6 months	-	-

Table 1: The timeline of JET experiments between 2021 and 2023. The measurements of the radiation effect on the test fibre were performed during DTE2 and DTE3

At the beginning of the DTE2 campaign before the optical transmission of the fibre assembly was significantly affected, measurements of the radiation induced emission were taken. Afterwards, the optical transmission was monitored in selected pulses throughout DTE2. Data from 167 different pulses was recorded, with generated fusion energy in each pulse ranging from near zero to the highest achieved in the campaign.

At the beginning of DTE3 campaign, the setup was reconfigured to only measure the couple of radiation resistant OH-doped fibres, identical to those used to connect the sample 60m pure silica fibre to the lab. Six pulses were measured, with neutron production in a rather narrow range of 2.1-2.9*10^{18} per pulse. The setup was then reconfigured back to the default state and further 30 measurements were taken.

Numerous experiments in pure deuterium plasmas were done at JET between DTE2 and DTE3, as well as preceding the JET closure at the end of 2023. The test fibre was not moved from its location during that time and no transmission measurements were taken. The total amount of neutrons produced by JET in these two periods constituted only a small fraction of those during DTE2+DTE3 (see Table 1) and the vast majority of the neutrons produced were from D-D reactions and had much lower energy. The radiation damage accumulated in the test fibre during the periods of pure D experiments is therefore negligible in comparison with the D/T campaigns.

Radiation-induced emission.

With the light source switched off in the experimental setup, only the radiation-induced emission produced by the fibres during JET pulses is detected. Figure 2 shows an example of this measurement done during JET pulse #99351 (9.0*10^{17} neutrons produced).

On Figure 2a the raw spectrum is plotted (blue) as measured by the spectrometer, together with the sensitivity calibration curve (black) and the calibrated spectrum (red). The calibration curve is derived by observing the calibrated light source placed on JET via a single OH-doped fibre. The emission spectrum at λ>550nm approximately follows the $1/\lambda^3$ dependence characteristic for Cherenkov radiation, according to the Frank-Tamm equation (1) but deviates from it at shorter wavelengths.

$$\frac{\partial^2 E}{\partial x \partial \lambda} = \pi c^2 e^2 \mu_W(\lambda) \frac{1}{\lambda^3}\left(1 - \frac{1}{\beta^2 n^2(\lambda)}\right) \tag{1}$$

On Figure 2b, the intensity of the radiation induced emission, integrated over the wavelengths λ=450-700nm is plotted versus time (1 second time resolution), overlaid with JET neutron emission measurements. The time evolution closely follows neutron emission with no afterglow visible on that time scale.

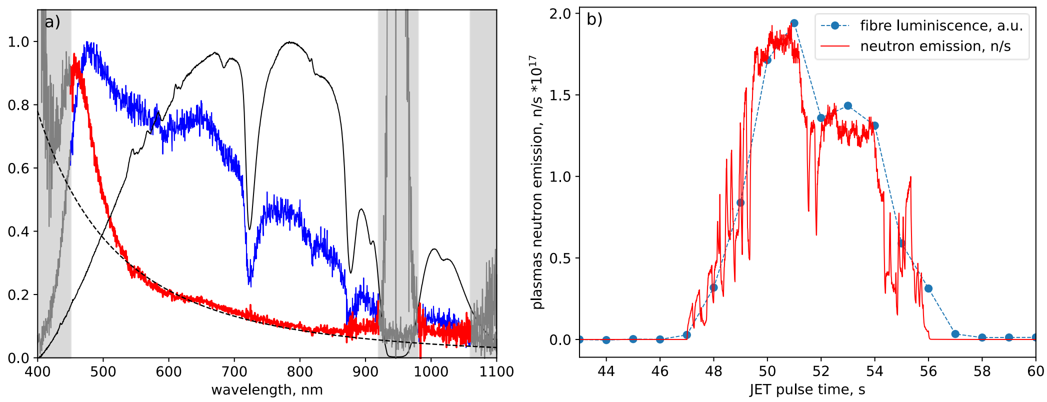

Figure 2; a) raw spectrum (blue), calibration curve (black) and calibrated spectrum (red) of the radiation induced emission measured during JET pulse 99351. Dashed line represents ~1/λ^3
b) time evolution of the emission (1 second per frame) versus time trace of neutron production rate during the pulse.

Short-term radiation-induced absorption

Each measurement in this setup consisted of 600 frames, with the first ~40 frames representing the initial spectral transmission just before JET pulse, 1-10 frames of rapid evolution during the neutron irradiation and the rest of the measurement shows the relaxation period. The absolute level of the signal depends on the spectral interval of interest and on the time period when the measurement has been made, as the permanent loss of fibre transmission slowly accumulated throughout the DT experiments. Therefore we show the data in the form of transmission loss with respect to the level measured immediately prior a JET pulse: T(dB)= $10*\log_{10}(S_i/S(t))$ where the initial signal level S_i will be taken from the first 20 frames.

On Figure 3 an example of the measurement is shown, taken during the JET highest fusion yield pulse #104522 (E_{fus}=69MJ or $2.46*10^{19}$ DT neutrons). Time trace starts at zero value, as this was chosen as the reference level. At the time when a significant amount of fusion power starts to be released, the attenuation is measuring negative values (signal increases), as radiation-induced emission exceeds the reduction of the probing light intensity from the induced transmission loss. As pulse progresses and the radiation damage in the fibre accumulates, transmission loss overtakes the emission and the measured attenuation reverses sign. At the end of the JET pulse the radiation-induced emission disappears, and the attenuation shows the highest value at that point. During the following ~9 minutes a part of the transmission loss is recovered due to self-annealing. The time evolution of the recovery can be fitted with a “stretched exponential” function (2), as observed in the past in numerous other experiments ([1,9])

$$S = T_1 * \exp\left(-\left(\frac{t}{\tau}\right)^{\alpha}\right) + T_2 \quad (2)$$

Here T_1 corresponds to the transient transmission loss which recovers after a period of time, and T_2 is the permanent damage. Note that the fitted T_2 is larger than the long-term

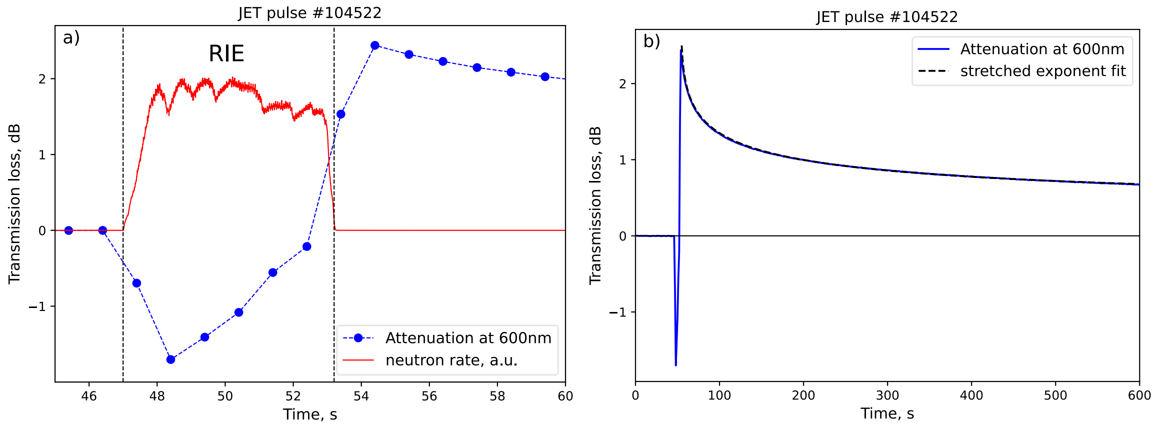

Figure 3 a) Measured attenuation in the fibre during JET pulse #104522, at λ=600nm

b) Time evolution of the measured optical transmission loss in the fibre assembly, Stretched exponential fit defined by equation (2) with parameters: τ=24.4s, α=0.28, T_1=3.17, T_2=0.39

transmission loss calculated from the trend observed throughout the DTE2, as it will be shown later in this paper. Parameters τ and α define the time evolution of the transmission post-irradiation. The strength of the transient transmission loss depends on the number of fusion neutrons produced in a particular pulse, but also different at different wavelength. On Figure 4a the transient transmission loss – defined at the maximum observed attenuation during JET pulse (typically it’s the measurement immediately after the end of high neutron flux period, see figure 3b), versus total number of neutrons produced in a pulse. The dependence is nearly linear over 2 orders of magnitude of the dose received. Linear fit of the data suggests that the dose corresponding to $1*10^{19}$ neutrons produced in JET would result in the following transient attenuation: **1.19dB at 600nm, 0.44dB at 800nm and 0.3dB at 1025nm.** Some scatter in the points and the deviation from the linear dependence towards the highest dose rate most likely caused by different duration of the irradiation, as the high-power phase could last between 1 and 6 seconds, thus the accumulation of the dose in longer pulses competes with self-annealing of the damage which happens in parallel. It can be seen on figure 3b that a non-negligible recovery of transmission can happen even at 1 second time scale. As it was mentioned earlier, in addition to the complete setup (60m test fibre + radiation resistant transfer fibres) a measurement of only OH-doped fibres has also been performed to exclude the contamination of results. Somewhat surprisingly, the transient transmission loss in the transfer line appeared to be non-negligible, and at λ>800nm even dominated the total transmission loss of the setup. Figure 4b shows the comparison of the transient transmission loss versus wavelengths for both cases, all 6 measurements of high-OH fibres (blue) overlaid with other 6 measurements of the complete setup, pulses chosen to be in a similar neutron dose range. This result suggests that at ~700nm the transient RIA in the fused silica sample is similar to that in the high-OH fibre, and at λ>800nm the short-

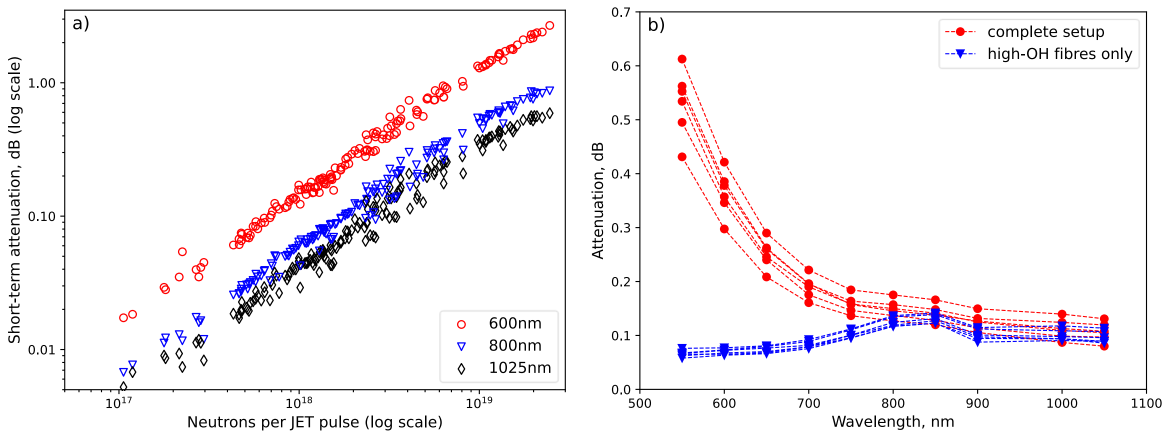

Figure 4 a) prompt attenuation measured as a function of the total number of neutrons produced in JET pulses, at 3 different wavelength ranges with +/-25nm averaging window: 600nm, 800nm and 1025nm. Combined DTE2+DTE3 dataset.

*b) attenuation versus wavelength, measured in the complete setup and in the transfer high-OH fibres only. ~2.5*10^{18} neutrons produced in each case.*

term RIA of this fibres setup comes predominantly from the high-OH.

Long-term radiation damage

In each recorded transmission measurement, first ~40 frames show the state of the transmitted signal prior to a JET pulse. At least 40 minutes normally passes between subsequent JET pulses and practically all the short-term RIA recovers in that time. By monitoring the intensity of the probing signal prior to each JET pulse throughout the DT campaigns we could document the evolution of the long-term radiation induced damage to the overall setup. The results are shown in figure 5.

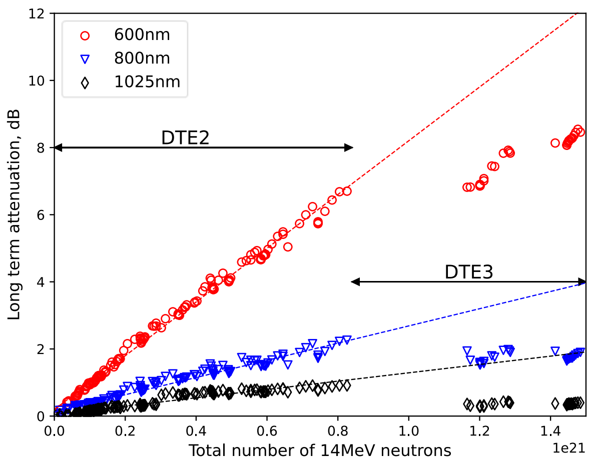

Figure 5: Long term attenuation at three spectrum intervals (600nm, 800nm, 1025nm with +/-25nm averaging) versus total number of 14MeV neutrons produced. Dashed lines represent linear fit of DTE2 data

During DTE2, radiation induced accumulation of the transmission loss is proportional to the dose. Linear fit of the data suggests that the dose corresponding to 1*10^{19} neutrons produced in JET would result in the following long-term attenuation: **0.08dB at 600nm, 0.026dB at 800nm and 0.012dB at 1025nm.** Comparing with the numbers found for the short-term effect, we conclude that 94-96% of the prompt transmission loss is eventually recovered.

Notably, the data measured in the subsequent DTE3 campaign doesn't follow the trend of the DTE2. This is most likely due to a combination of two reasons: 1) as the configuration of the setup has been modified early in DTE3 to only measure the high-OH fibres, the reconnection may have changed (improved) the coupling of fibres resulting in the overall apparent reduction of attenuation; and 2) the self-annealing of the radiation induced damaged continues on a very long timescale, so some of the radiation damage accumulated during the DTE2 was recovered by the time the DTE3 experiments took place.

Approximately 8 months after the end of DTE3 campaign, the fibre sample has been removed from JET and its optical transmission was measured by comparison with an identical 60m fibre which has not been irradiated. The results are shown in figure 6.

If we assume that the long-term RIA is proportional to the short-term effect, then the data on figure 6 is consistent with figure 4b – namely that the observed attenuation in longer wavelengths λ>800nm is predominantly from the high-OH fibres used for transmitting light between JET and the lab, and at <700nm attenuation in the low-OH sample is dominant.

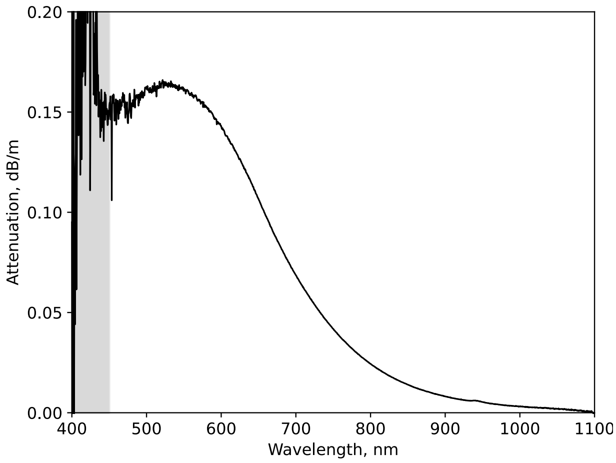

Figure 6: Final long-term attenuation in the low-OH 60m fibre measured ex-situ.

Irradiation dose

The coupled neutron/gamma MCNP simulation was run to calculate the fluence at the location of the low-OH fibre. The results showed that the neutron fluence is $2.53*10^{-8}$n/cm^2 per neutron emitted by JET, of these $1*10^{-8}$n/cm^2 are high energy neutrons (E>0.1MeV). Total gamma photon fluence is around 1/3rd of the total neutron fluence. The total number of 14.1MeV neutrons produced during the DTE2 and DTE3 campaigns is ~$1.58*10^{21}$, therefore the total neutron fluence on the fibre is $4*10^{13}$n/cm^2. Spectrum of the neutrons and gammas at the location of the fibre is shown in figure 7. The absorbed dose in the fibre is calculated with Fispact-II code [11], using SiO_2 as absorbing material and neutron/gamma spectra as predicted by MCNP. The result absorbed kerma dose in the fibre from the neutron irradiation is ~300Gy, and from gammas ~35Gy

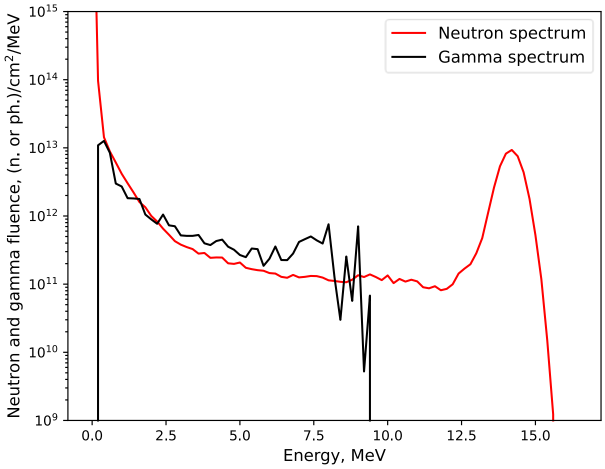

Figure 7: total neutron and gamma fluence spectrum at the location of the sample fibre calculated by MCNP

Discussion and conclusions

At the planning stage of this experiment, we expected that the radiation effects in the OH-doped fibre will be minor. The outcome was somewhat surprising, as in the near-infrared range of spectrum the situation appeared to be opposite. But we shall caution the reader from making conclusions on the effect of OH-doping on the radiation hardening of fibres, as the two types of fibres used in this setup came from different sources and at different times, i.e. there could be multiple other factors in play.

One of the goals of this work is to quantify the effect of radiation on the performance of the Thomson Scattering diagnostic (HRTS) used at JET. The diagnostic uses 1064nm laser for the measurement, and the scattered spectrum is in the range of λ=650-1060nm with signals in the shortest wavelengths only coming from the hottest electrons the in the very plasma core. Given that the length of the test fibre was at least 6 times longer and it was positioned in a way to get several times larger neutron flux, the conclusion is that the effect on the actual diagnostic was negligible.

Radiation-induced emission is believed to be attributed to Cherenkov radiation caused by fast electrons travelling through the fibre media. We did the measurement with high spectral resolution in the visible range and did not observe any line emission. The emission largely follows the $1/\lambda^3$ trend except in the shortest wavelengths. Unfortunately, in this setup it was not possible to quantify the absolute intensity of the emission.

Observation of the prompt (short-term) radiation induced attenuation is consistent with previous works, including the self-annealing of around 95% of the initial damage at room temperature [1]. In this work we explored the wavelength dependence in the visible and near-infrared range. At shorter wavelength (λ<600nm) the prompt attenuation appears to be stronger in the low-OH fibre than in the high-OH, and at the longer wavelength (λ>800nm) we observed the opposite – the radiation resistant fibre appeared to be more susceptible to radiation-induced attenuation than the pure SiO_2 fibre.

The self-annealing at room temperature follows a stretched exponential decay, indicating that at least some of the radiation-induced darkening is coming from some sort of recombination or bi-molecular process (discussed in [9]). It means the rate of the short-term damage recovery must depend on the density of the radiation-induced defects, therefore irradiation of a long fibre with a lower neutron flux might have a different recovery rate in comparison with a shorter fibre under a higher intensity neutron flux, which is likely the case for applications in the future DT fusion facilities.

The long-term attenuation appears to be roughly proportional to the short-term effect (compare the red curves on figure 4b and figure 6). It is especially strong at λ=500-600nm and this is where OH-doping of the fibres appears to make the biggest difference. Near 1000nm the residual transmission loss of the pure SiO_2 test fibre of 60 metres length is only 5%. Even unheated low-OH pure SiO_2 fibre showed remarkable resistance to radiation at λ>800nm, so a Thomson Scattering system measuring mild range of electron temperatures would likely not require special fibres, especially if fibre heating is implemented.

Calculated total absorbed dose from neutrons during the whole exposure period (DTE2+DTE3) is ~300Gy, which caused a long-term RIA of the low-OH sample fibre of 0.15dB/m in the 500-600nm range and ~0.015dB/m at 850nm. The dose associated with gamma radiation in this experiment was found about an order of magnitude lower.

Note that the neutron kerma dose is calculated as deposition of energy in pure SiO_2. It has been shown in [13] that the actual dose in the fibre core can be significantly higher due to the recoil protons from the fibre cladding. The actual neutron dose amplification depends on the cladding material and configuration of the fibres, the numbers quoted in [13] range from 20% to 175% for 14.1MeV neutrons, where lower value corresponds to single fibre and higher to tightly packed fibre bundles. It is not possible to estimate the amplification factor in the fibre used in this work. With that in mind, the real deposited dose in the tested fibre can be anywhere between 300-700Gy.

As reported in [6], irradiation of 4m low-OH fibre with gamma dose of 10kGy results in 7dB transmission loss at λ~550nm, or 0.05 dB/m equivalent for 300Gy. Factor of 10 less RIA was measured at λ>850nm for the same irradiation dose. In [13] for a pure SiO_2 low-OH fibre, RIA of ~0.17dB/m at λ~550-650nm is reported after 200Gy gamma dose, although the observed attenuation at longer wavelengths was significantly larger than observed here and in [6], of the order of 0.05-0.1dB/m

Comparison of radiation induced damaged caused to optical fibres by 14MeV neutron and gammas has been done in [12] with the conclusion that the effect is similar for the same absorbed dose. We can conclude that with some uncertainty of factor 1-2, our observations of long-term RIA are more or less consistent with the published results obtained with gamma irradiation, therefore confirming the findings of [12]

Acknowledgments

This work has been carried out within the framework of the EUROfusion Consortium, funded by the European Union via the Euratom Research and Training Programme (Grant Agreement No 101052200 — EUROfusion) and from the EPSRC [grant number EP/W006839/1]. To obtain further information on the data and models underlying this paper please contact PublicationsManager@ukaea.uk*. Views and opinions expressed are however those of the author(s) only and do not necessarily reflect those of the European Union or the European Commission. Neither the European Union nor the European Commission can be held responsible for them.

References

[1] A.T. Ramsey et al., Review of Scientific Instruments 68, 632 (1997); https://doi.org/10.1063/1.1147670
[2] A.C. Maas et al., Fusion Engineering and Design 47 (1999) 247–265
[3] H. Henschel et al., IEEE Transactions on Nuclear Science (Volume: 41, Issue: 3, June 1994), pages 510-516, DOI: 10.1109/23.299791
[4] Jicong Li et al., Sensors 2024, 24(10), 3235; https://doi.org/10.3390/s24103235
[5] B. Brichard et al., Journal of Nuclear Materials 329–333 (2004) 1456–1460
[6] R. Scannell et al 2017 JINST 12 C11010, DOI: 10.1088/1748-0221/12/11/C11010
[7] R. Pasqualotto et al., Rev. Sci. Instrum. 75, 3891–3893 (2004) https://doi.org/10.1063/1.1787922
[8] B. W. Brown et al., Rev. Sci. Instrum. 66, 3077–3078 (1995)
[9] D. L. Griscom et at., Phys. Rev. Lett. 71, 1019, doi: https://doi.org/10.1103/PhysRevLett.71.1019
[10] C.J. Werner (editor), MCNP Users Manual - Code Version 6.2, LA-UR-17-29981, 2017
[11] J.-C. Sublet , J.W. Eastwood , J.G. Morgan , M.R. Gilbert , M. Fleming , W. Arter , FIS-PACT-II: an advanced simulation system for activation, transmutation and material modelling, Nucl. Data Sheets 139 (2017) 77–137.
[12] H. Henschel et al., "Comparison between fast neutron and gamma irradiation of optical fibres," RADECS 97. Fourth European Conference on Radiation and its Effects on Components and Systems (Cat. No.97TH8294), Cannes, France, 1997, pp. 430-438, doi: 10.1109/RADECS.1997.698960
[13] B. R. L. Siebert and H. Henschel, "Calculation of fast neutron dose in plastic-coated optical fibres," RADECS 97. Fourth European Conference on Radiation and its Effects on Components and Systems (Cat. No.97TH8294), Cannes, France, 1997, pp. 466-471, doi: 10.1109/RADECS.1997.698974.
[14] A. Gusarov et al., Fusion Engineering and Design, vol. 151, 2020 https://doi.org/10.1016/j.fusengdes.2019.111356